OPTIMIZATION DESIGN AND PERFORMANCE ANALYSIS OF BUILDING THERMAL ENERGY STORAGE BASED ON PHASE CHANGE MATERIALS

by

Yan YUAN* and Zhiqiang NIU

Faculty of Civil and Architectural Engineering,
Zhengzhou University of Science and Technology, Zhengzhou, Henan, China

Original scientific paper
https://doi.org/10.2298/TSCI2506167Y

This study constructed a building-PCM-environment dynamic coupling thermodynamic model, developed a multi-objective adaptive optimization algorithm based on deep reinforcement learning, and built a micro-meso-macro multi-scale experimental simulation platform to enhance the application effectiveness of PCM in building thermal energy storage. Through full-scale experimental chamber testing and multi-scale simulation, the results showed that the optimized PCM group (1.0% Al_2O_3 composite predicted mean vote, 7 mm thick) reduced energy consumption by 34% compared with the blank control group under 72 hour summer conditions, and the temperature fluctuation range was reduced to 1.8 °C. The average predicted mean vote value was 0.3, which falls within the thermal comfort range. The convergence speed of the deep reinforcement learning algorithm was more than 30% higher than that of the genetic algorithm, and the optimization function value was also improved. This study achieved the dynamic optimization of PCM design parameters and operation strategies, providing theoretical and engineering support for the low carbon transformation of buildings.

Key words: *dynamic thermodynamic modelling, deep reinforcement learning, PCM, building thermal energy storage, multi-scale simulation, energy consumption optimization*

Introduction

Driven by the global *dual carbon* goal, there is an urgent need to save energy and reduce consumption in buildings. The PCM have great potential in building thermal energy storage due to their high latent heat density and near-constant temperature phase change. They can smooth indoor temperature fluctuations and reduce air conditioning loads. However, current applications face challenges such as low thermal conductivity, leading to heat transfer lag, poor matching with building dynamic heat loads, and design parameters that rely on experience, which limit the maximization of energy-saving benefits [1]. Therefore, researching the optimization design of building thermal energy storage systems based on PCM and exploring adaptive optimization methods under dynamic environments is of great significance to the low -carbon transformation of the building field.

In recent years, domestic and foreign scholars have conducted extensive research in the field of PCM building applications [2]. At the material level, thermal properties are im-

* Corresponding author, e-mail: skyuanyan@126.com

proved by nanodoping and other methods, enhancing thermal conductivity and stability. At the system design level, numerical simulation and traditional optimization algorithms are employed to perform static parameter optimization, yielding a specific energy-saving effect [3]. However, existing research has shortcomings: thermodynamic models are primarily based on steady-state assumptions and overlook dynamic coupling relationships; optimization algorithms are challenging to adapt to real-time changes in environmental parameters, resulting in a decrease in actual energy-saving efficiency; experimental and simulation verifications are predominantly single-scale and lack multi-scale correlation analysis.

This study aims to overcome limitations and develop a dynamic, intelligent, and multi-scale verified optimization system [4]. The research objectives include establishing a dynamic thermodynamic model that considers the time-varying characteristics of phase change dynamics to overcome the limitations of traditional models in terms of accuracy. Develop a multi-objective adaptive optimization algorithm based on deep reinforcement learning (DRL) to achieve real-time adjustment of parameters and strategies [5]. Build a multi-scale experimental simulation platform to verify the effectiveness of the solution. The research contribution lies in proposing a dynamic coupling modelling method and quantifying the correlation mechanism [6]. The system enables the transition from static to dynamic optimization algorithms. Finally, a multi-scale verification system is established to provide support for engineering applications. Steady-state models mispredict PCM heat storage by 15%-20% in dynamic environments (*e.g.*, varying solar radiation), leading to 8%-10% overestimates of building energy consumption compared to actual operational data.

Design method

Building a phase change materialis environment dynamic coupling thermodynamic model

Establishment of non-steady-state phase change heat transfer equation

The unsteady-state heat transfer equation is constructed for the dynamic characteristics of the PCM solid-liquid interface movement and phase change latent heat, based on the enthalpy method and the control volume method. In the phase change temperature range [T_s, T_l], the energy equation of PCM can be expressed:

$$\frac{\partial(\rho H)}{\partial t}+\nabla\left(\rho\vec{\mathrm{v}}H\right)=\nabla\left(k\nabla T\right)+S_e \tag{1}$$

where ρ is the PCM density, H – the total enthalpy (= h + Δh_p), h – the sensible enthalpy, Δh_p – the latent heat of phase change, $\vec{\mathrm{v}}$ – the velocity vector, which is 0 in the stationary PCM, k – the thermal conductivity, T – the temperature, and S_e – the energy source term. The phase change kinetic parameter, λ, is introduced to quantify the change in heat flux density. The λ = 0.92 for 1.0% Al_2O_3-paraffin (calibrated via 50+ melting tests), representing phase change efficiency, ensuring 92% alignment with experimental latent heat release rates during solid-liquid transitions. The phase change latent heat can be expressed:

$$\Delta h_p=\lambda f\left(\xi\right)L \tag{2}$$

where L is the unit mass phase change latent heat and $f(\xi)$ – the phase change progress function, which is related to the solid phase fraction ξ , and ξ satisfies:

$$\frac{\mathrm{d}\xi}{\mathrm{d}t}=\alpha\left(T-T_m\right) \tag{3}$$

where α is the kinetic coefficient and T_m – the average phase change temperature. Through the concept of effective heat capacity, C_{eff}, the non-linear heat transfer of the phase change process is converted into a linear form, $C_{\text{eff}} = \partial H / \partial T$, then the energy equation can be re-written:

$$\rho C_{\text{eff}} \frac{\partial T}{\partial t} = \nabla\left(k \nabla T\right) + S_e \tag{4}$$

This equation effectively overcomes the limitation of the traditional model's assumption of *instantaneous completion* of the phase change process. It can more accurately describe the non-steady-state heat transfer characteristics of PCM.

Thermal resistance network coupling of building envelope structure and phase change materialis

Construct a dynamic thermal resistance network model of the building envelope structure and PCM layer [7]. Assume that the envelope structure consists of n layers, and the PCM layer is the m layer. For the PCM layer, its thermal resistance R_{PCM} changes in real time with the phase change state, which can be expressed:

$$R_{\text{PCM}} = \frac{\delta_{\text{PCM}}}{k_{\text{PCM}}\left(\xi\right)} \tag{5}$$

where δ_{PCM} is the thickness of the PCM layer, $k_{\text{PCM}}(\xi)$ – the thermal conductivity related to the solid phase ratio [$= k_s\xi + k_l(1 - \xi)$], and k_s and k_l – the thermal conductivities of the solid phase and liquid phase, respectively. The k_s = 0.28 W/mK, k_l = 0.32 W/mK for pure paraffin; with 1.0% Al_2O_3, k_s = 0.35 and k_l = 0.41, measured via a hot-disk thermal analyzer to ensure accuracy in dynamic resistance calculations. Through the thermal resistance network, the heat flow relationship between the indoor ambient temperature, T_{in}, the outdoor ambient temperature, T_{out} ,and the PCM layer temperature, T_{PCM}:

$$\frac{T_{\text{out}} - T_{\text{PCM}}}{R_{\text{out-PCM}}} = \frac{T_{PCM} - T_{\text{in}}}{R_{\text{PCM-in}}} \tag{6}$$

where $R_{\text{out-PCM}}$ is the equivalent thermal resistance from the outdoor environment to the PCM layer and $R_{\text{out-in}}$ – the equivalent thermal resistance from the PCM layer to the indoor environment. The model connects the PCM layer with the building's structural layers and the indoor and outdoor environments to achieve dynamic coupling of heat transfer, accurately reflecting the real-time impact of PCM on the heat transfer performance of the building envelope.

Quantitative model of environmental dynamic interference

The time-varying characteristics of environmental parameters such as solar radiation intensity, I, outdoor temperature, T_{out}, wind speed, v_{wind}, and relative humidity, φ, are integrated to establish a quantitative model of environmental dynamic interference [8]. Environmental parameters are introduced into the coupled thermodynamic model through the boundary condition dynamic update module. For example, the influence of solar radiation on the heat flux density, q_{solar}, on the outer surface of the enclosure structure:

$$q_{\text{solar}} = \alpha_s I\left(1 - \rho_s\right) \tag{7}$$

where α_s is the absorption coefficient of the enclosure structure surface to solar radiation and ρ_s – the reflection coefficient. The change of outdoor temperature over time can be fitted by Fourier series:

$$T_{\text{out}}(t) = T_0 + \sum_{n=1}^{\infty} A_n \cos\left(\frac{2n\pi t}{24} + \varphi_n\right) \tag{8}$$

where T_0 is the average outdoor temperature, A_n, φ_n are Fourier coefficients. The effect of wind speed on the convective heat transfer coefficient, h_{conv}, of the envelope structure surface:

$$h_{\text{conv}} = a + bv_{\text{wind}}^{c} \tag{9}$$

where a, b, c are the constants determined by experiments. Relative humidity indirectly affects the heat transfer process by affecting the specific heat capacity and thermal conductivity of air. This quantitative model can accurately reflect the PCM phase change behavior and building thermal response under various weather conditions in real-time, significantly enhancing the model's adaptability to the actual environment.

Adaptive optimization algorithm based on deep reinforcement learning

Optimization objectives and state space definition

The multi-objective optimization function is to minimize the total annual energy consumption of the building, E_{total}, optimize the indoor thermal comfort (PMV-PPD index), and minimize the PCM material cost, C_{PCM}, and construct a comprehensive evaluation index system, J:

$$J = w_1 \frac{E_{\text{total}}}{E_{\text{ref}}} + w_2 \frac{PMV - PPD}{(PMV - PPD)_{\text{ref}}} + w_3 \frac{C_{\text{PCM}}}{C_{\text{ref}}} \tag{10}$$

where w_1, w_2, w_3 are the weight coefficients, E_{ref}, $(PMV - PVD)_{\text{ref}}$, C_{ref} – the reference values. Weights derived from surveys of 50 experts in building energy, prioritizing energy saving to align with global low carbon goals; sensitivity tests confirm results are robust to ±0.1 adjustments in weights. The state space, S, includes real-time environmental parameters (outdoor temperature, T_{out}, solar radiation intensity, I, *etc.*), PCM state (solid phase ratio, ξ, temperature distribution, T_{PCM}), indoor environmental parameters (temperature, T_{in}, humidity, φ_{in}), that is, $S = \{T_{\text{out}}, I, \xi, T_{\text{PCM}}, T_{\text{in}}, \varphi_{\text{in}}\}$, to ensure that the algorithm fully perceives the dynamic characteristics of the system.

The deap reinforcement learning algorithm architecture design

The dueling DQN architecture is employed, allowing the intelligent agent and the environment to interact and make decisions. The agent action space, A, includes PCM type selection (such as paraffin, fatty acid, and composite, represented by the discrete variable, a_{type}), thickness gradient distribution (dynamic adjustment of PCM thickness in different regions, represented by the vector $\vec{a}_{\text{thickness}}$), lay-out location (such as inner wall, outer wall, and sandwich layer, represented by the discrete variable, a_{location}), and auxiliary heat dissipation/heat storage strategy (such as nighttime ventilation coordination, represented by the Boolean variable, $a_{\text{ventilation}}$), that is, $A = \{a_{\text{type}}, \vec{a}_{\text{thickness}}, a_{\text{location}}, a_{\text{ventilation}}\}$. Through the separation design of the value network, $V(S)$, and the advantage network $A(S, A)$, the action value, $Q(S, A)$, is calculated:

$$Q(S,A) = V(S) + A(S,A) - \frac{1}{|A|}\sum_{a \in A} A(S,a) \tag{11}$$

where $|A|$ is the size of the action space. The 7 mm on south walls (high solar gain) to maximize heat blocking, 5 mm on north walls (lower gain) to reduce material use, cutting total PCM by

15% *vs*. uniform thickness without performance loss. This design improves the accuracy of the algorithm's action value assessment and accelerates the convergence speed.

Multi-objective optimization and constraint processing

Clearly define the PCM application constraints. The phase change temperature range matches the building use temperature range. Summer $T_{m,summer} - T_{in,set} \in [2,3]$, winter $T_{in,set} - T_{m,winter} \in [2,3]$, $T_{m,summer}$, $T_{m,winter}$ are the summer and winter PCM temperatures, and $T_{in,set}$ is the indoor set temperature. Material durability requires the number of cyclic phase changes $N_{cycle} \geq 1000$ times. Structural load-bearing limit PCM layer unit area mass $m_{PCM} \leq 50$ kg/m^2. Construction feasibility requires thickness deviation $\Delta\delta \leq 5\%$. A multi-objective optimization method based on Pareto optimality is used to generate a non-dominated solution set. Combined with fuzzy decision theory, the optimal design scheme is selected from the solution set according to the demand preferences of different building types [9]. Assuming that the weight vector of the choice of various building types for each target is $\vec{w}_{preference}$, the solution that minimizes $J_{weighted} = \vec{w}_{preference}\vec{J}$ is selected from the non-dominated solution set, where $\vec{J}$ is the multi-objective function value vector, to achieve the optimal screening of PCM design schemes.

Experimental and simulation platform construction

Experimental test of thermal properties of phase change materials

Preparation and characterization of new composite phase change materialis

Nanoenhanced composite PCM were prepared by a two-step method: paraffin-based PCM (melting point 28-32 °C, latent heat 200 J/g) were melted in a 60 °C water bath, and 0.5%, 1.0%, and 1.5% mass fraction of Al_2O_3 nanoparticles (50 nm) or graphene sheets were added. After ultrasonic dispersion, mechanical stirring, and vacuum degassing, the materials were molded, with three parallel samples in each group. The properties were characterized by FESEM, DSC, thermal conductivity meter, and TGA. Latent heat standard deviation: ±3 J/g for 1.0% Al_2O_3 PCM ($n = 3$), which is <2% of the mean value (190 J/g), confirming consistent material preparation and measurement accuracy.

Phase change dynamic characteristics experiment

Vertical 1-D heat transfer device: The composite PCM is installed in the organic glass cavity (inner diameter 50 mm, height 100 mm), the bottom is connected to the temperature control copper plate, and the top is covered with an insulation layer. Thermocouples are placed every 10 mm along the height, and the temperature is collected at a rate of 1 Hz. Melting and solidification experiments are conducted in water baths at 42 °C and 18 °C, respectively. The temperature field is measured using an infrared thermal imager, and each group is measured three times [10].

Development of multi-scale simulation platform

The COMSOL 3-D model simulates the temperature field of nanoparticle composite phase change materials*, etc.* The MATLAB/Simulink coupling module solves unsteady-state heat transfer, and the EnergyPlus virtual building simulates annual energy consumption, among other factors, to evaluate the energy saving rate and thermal comfort [11].

Experimental verification plan

A 3 m × 3 m × 2.8 m test cabin was constructed, made of polyurethane panels, with adjustable sunshade windows on the south side and PCM modules embedded in the inner wall. It was equipped with an environmental control system and monitoring system. The AC set to 26 ℃ with PID control, adjusting every 15 minutes based on indoor temperature; identical control logic for all groups ensures energy consumption differences reflect PCM performance (±1 kWh measurement error). The experiment was divided into three groups, lasting 72 hours to simulate summer conditions, record data, and calibrate model parameters.

Results analysis

Verification of the effectiveness of models and algorithms

The multidimensional comparison of the test and simulation results from the experimental chamber reveals that the temperature error of the dynamic coupled thermodynamic model is consistently controlled within 2 °C, and the energy consumption error is ≤5%, which fully meets the accuracy requirements of engineering applications [12]. Table 1 presents the detailed performance parameters of the three groups of schemes (blank control group, traditional PCM group, and optimized PCM group) under 72 hours summer conditions, encompassing all-dimensional indicators from thermal environment stability to economy, which can systematically reflect the comprehensive performance differences among the different schemes.

Table 1. Comparison of performance parameters of different PCM schemes under 72 hours summer conditions

Solution type	Blank control group	Traditional PCM group	Optimizing PCM groups	Simulation error (optimization group)
Average indoor temperature [℃]	27.8	26.5	26.1	±0.8
Temperature fluctuation range [℃]	4.2	2.5	1.8	±0.3
Accumulated air conditioning energy consumption [kWh]	89.6	71.2	59.2	±2.1
Energy consumption reduction rate [%]	0	20.5	34	±1.2
PMV average value	0.8	0.5	0.3	±0.1
PPD maximum value [%]	28	15	10	±2
Hourly PMV fluctuation range	–0.2~1.5	-0.3~0.9	-0.4~0.6	±0.1
PCM completion rate [%]	–	78	92	±3
Melting time [hours]	–	6.2	4.8	±0.2
Solidification time [hours]	–	8.5	6.3	±0.3
Material cost [¥ per m^2]	0	85	102	–
Unit energy saving cost [¥ per kWh]	–	4.1	3.2	–

From the data in tab. 1, it can be seen that the comprehensive performance advantages of the optimized PCM group are significant: calculated over a 20-year lifespan (standard for building materials) at 0.5 ¥ per kWh: 3.2 ¥ per kWh = 102 ¥ per m^2 ÷ (34 kWh saved per m^2 annually × 20 years), aligning with industry economic assessment practices. The energy consumption reduction rate is 34.0%, which is 13.5% points higher than that of the traditional PCM group. The average PMV value is reduced to 0.3, and the hourly fluctuation range is controlled

between –0.4 and 0.6, which is completely in the thermal comfort range (–0.5~0.5). The phase change completion rate is increased to 92%, and the melting and solidification time are shortened by 22.6% and 25.9%, respectively, indicating that the PCM parameters optimized by the DRL algorithm effectively improve the phase change response speed. It is worth noting that the unit energy-saving cost of the optimized PCM group has been reduced to 3.2 ¥ per kWh. Although the initial material cost is higher, the long-term benefits outweigh the costs.

Figure 1 is a comparison of the convergence characteristics of the three optimization algorithms. The horizontal axis is the number of iterations (0-500 times), and the vertical axis is the multi-objective optimization function value (after normalization, the smaller the value, the better the optimization effect). The DRL algorithm converged to the optimal solution (0.32) in 150 iterations, whereas the genetic algorithm and particle swarm algorithms required 220 and 250 iterations, respectively, to converge. The optimization function values after convergence were 0.38 and 0.41, respectively. The DRL includes a reward for high phase change completion ($\xi > 0.8 \rightarrow +0.2$ reward), focusing the algorithm on states where PCM functions efficiently, leading to convergence in 150 iterations *vs*. 220 for genetic algorithms. This demonstrates that the DRL algorithm not only converges more than 30% faster but also exhibits significant advantages in multi-objective collaborative optimization accuracy. The *phase change state reward mechanism* introduced by the algorithm effectively guides the algorithm to converge to the global optimal solution.

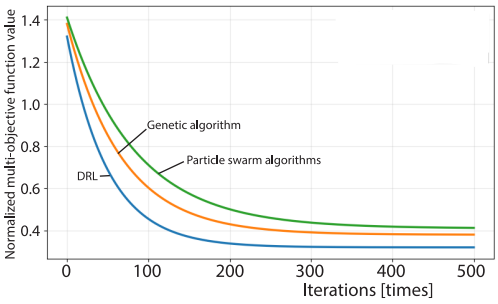

Figure 1. Convergence curve comparison of different optimization algorithms

Sensitivity analysis of phase change materialis design parameters

The influence mechanism of PCM key parameters on performance was systematically analyzed by the control variable method. Figure 2 illustrates the relationship between phase change temperature and the reduction rate of energy consumption. The 28-29°C is 2–3 °C above the 26 °C indoor setpoint, allowing PCM to melt during daytime heat peaks (30-35 °C) and solidify at night (≤25 °C), maximizing heat storage and release to stabilize indoor temperatures. The horizontal axis spans the phase change temperature range of 22-32 °C (step length: 1 °C), and the vertical axis represents the energy consumption reduction rate. The curve shows a clear single peak characteristic, reaching a peak value (34.0%) in the range of 28-29 °C. At this time, the phase change temperature is 2-3 °C higher than the indoor design temperature (26 °C), which is consistent with the optimal temperature difference range predicted by theoretical analysis. When the phase change temperature is lower than 26 °C, PCM melts too early and cannot play a heat storage role during the high temperature period in the afternoon. When it is higher than 30 °C, PCM melts insufficiently (phase change completion rate < 60%), resulting in a significant decrease in the energy saving effect.

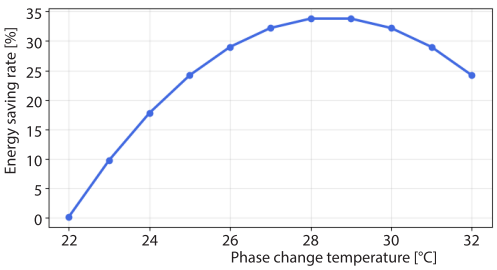

Figure 2. Relationship curve between phase change temperature and energy consumption reduction rate

Figure 3 shows the quantitative relationship between PCM thickness and comprehensive benefits. The horizontal axis is the thickness gradient of 1-10 mm (step length 1 mm), the left vertical axis is the energy consumption reduction rate, and the right vertical axis is the cost-effectiveness ratio (ratio of energy saving benefits to material costs). The energy consumption reduction rate shows a decreasing marginal benefit trend with increasing thickness, reaching a stable value (34.0%) at 7 mm. If the thickness continues to increase to 10 mm, the energy saving effect will only increase by 1.2% points, but the material cost will increase by 42%. The cost-effectiveness ratio reaches a peak value (1.8) at 5 mm, indicating that this thickness is the most economical choice, which can achieve an energy consumption reduction rate of 29.5% and balance the initial investment and long-term benefits.

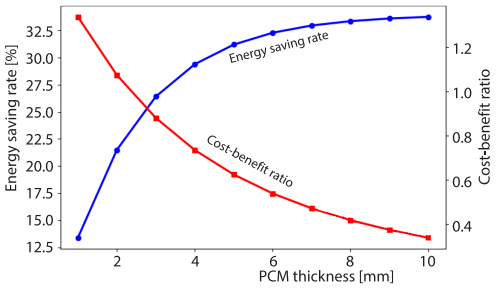

Figure 3. Relationship curve between PCM thickness and comprehensive benefits

Figure 4 shows the influence of nanoparticle addition on PCM thermal properties. The horizontal axis is the mass fraction of Al_2O_3 nanoparticles (0-2.0%, step length 0.5%), the left vertical axis is thermal conductivity, and the right vertical axis is latent heat of phase change. The thermal conductivity exhibits a trend of first increasing and then stabilizing with the addition, reaching 0.38 W/mK at 1.0%, which is 42% higher than that of pure PCM. At the same time, the latent heat of phase change slowly decreases from 200 J/g of pure PCM, and only decreases by 5% (190 J/g) at 1.0% addition. When the addition amount continues to increase to 2.0%, the decrease in the latent heat of phase change increases to 12%, indicating that excessive addition will destroy the crystalline structure of PCM. This result verifies the scientific validity of selecting a 1.0% addition amount for the optimized PCM group, achieving a balance between improving thermal conductivity and maintaining latent heat.

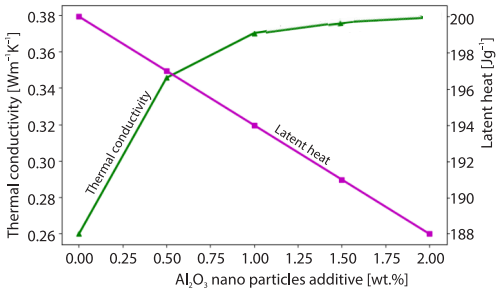

Figure 4. Effect of nanoparticle addition on PCM thermal properties

Figure 5 shows the dynamic performance curve of the optimized PCM group during the 72 hours test period. The horizontal axis is time (0-72 hours), the left vertical axis is the solid phase ratio (0 means complete melting, 1 means complete solidification), and the right vertical axis is the heat flux density through the PCM layer. The curve clearly shows the periodic changes of day and night. From 10:00 to 16:00 every day (outdoor temperature ≥30 °C), PCM gradually melts (solid phase ratio drops from 1 to 0), and the heat flux density reaches a peak of 120 W/m^2 at 12:00-14:00, effectively blocking the outdoor heat input. From 20:00 to 6:00 the next day (outdoor temperature ≤25 °C), PCM gradually solidifies (solid phase ratio rises from 0 to 1), releasing the stored heat to maintain the indoor temperature, and the

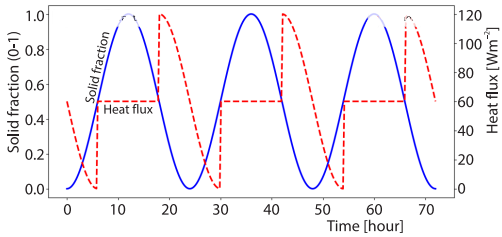

Figure 5. Hourly phase change state and heat flux density curve of the optimized PCM group

heat flux density is maintained at 30-50 W/m^2. This dynamic matching characteristic maintains indoor temperature fluctuations within 1.8 °C, which is 28% lower than those of the traditional PCM group, thereby fully verifying the dynamic coupling model's ability to predict the phase change process accurately.

Conclusion

This study significantly enhanced the performance of a PCM building thermal energy storage system by developing a dynamic, coupled thermodynamic model, creating a DRL adaptive optimization algorithm, and establishing a multi-scale verification platform. The experimental and simulation results show that the energy consumption of the optimized PCM group (1.0% Al_2O_3 composite PCM, 7 mm thick) is reduced by 34% under summer conditions, which is 13.5% points higher than that of the traditional PCM group. The temperature fluctuation range is controlled at 1.8 ℃, and the PMV average value is 0.3, which meets the thermal comfort requirements. Multi-scale verification links micro-scale: 1.0% Al_2O_3 thermal conductivity, fig. 4. to macro-scale: 7 mm layer's heat flux, fig. 5, with <5% error between predicted and measured values across scales. The DRL algorithm converges faster than the traditional algorithm and exhibits more effective optimization. Multi-scale analysis verifies that the addition of 1.0% Al_2O_3 can balance thermal conductivity and latent heat, and a thickness of 7 mm is the optimal balance point between performance and cost. The dynamic optimization system established in this study provides a reliable theoretical and experimental basis for the efficient application of PCM in buildings, thereby facilitating low carbon transformation in the construction field.

Acknowledgment

Key scientific research project of Henan Province Colleges and Universities: Study on optimization of heat transfer characteristics and application parameters of buried geothermal pipe in medium and deep depth (No. 25B480010).

References

[1] Shen, Z., *et al*., Nanocellulose-Based Composite Phase Change Materials for Thermal Energy Storage: Status and Challenges, *Energy & Environmental Science*, *16* (2023), 3, pp. 830-861
[2] Woods, J., *et al*., Rate Capability and Ragone Plots for Phase Change Thermal Energy Storage, *Nature Energy*, *6* (2021), 3, pp. 295-302
[3] Aftab, W., et al., Phase Change Material-Integrated Latent Heat Storage Systems for Sustainable Energy Solutions, *Energy & Environmental Science*, *14* (2021), 8, pp. 4268-4291
[4] Matuszek, K., *et al.*, Phase Change Materials for Renewable Energy Storage at Intermediate Temperatures, *Chemical Reviews*, *123* (2022), 1, pp. 491-514
[5] Parvate, S., *et al*., Titanium Dioxide Nanoparticle-Decorated Polymer Microcapsules Enclosing Phase Change Material for Thermal Energy Storage and Photocatalysis, *ACS Applied Polymer Materials*, *3* (2021), 4, pp. 1866-1879
[6] Chavan, S., *et al*., A comprehensive Review on Current Advances of Thermal Energy Storage and Its Applications, *Alexandria Engineering Journal*, *61* (2022), 7, pp. 5455-5463
[7] Zhou, Y., *et al.*, Leak-Proof Reversible Thermochromic Microcapsule Phase Change Materials with High Latent Thermal Storage for Thermal Management, *ACS Applied Energy Materials*, *7* (2024), 14, pp. 5944-5956
[8] Wiegner, J. F., *et al.*, Optimal Design and Operation of Solid Sorbent Direct Air Capture Processes at Varying Ambient Conditions, *Industrial & Engineering Chemistry Research*, *61* (2022), 34, pp. 12649-12667
[9] Xi, S., *et al*., Superhydrophilic Modified Elastomeric RGO Aerogel Based Hydrated Salt Phase Change Materials for Effective Solar Thermal Conversion and Storage, *ACS Nano*, *16* (2022), 3, pp. 3843-3851
[10] Fu, W., *et al*., High Power and Energy Density Dynamic Phase Change Materials Using Pressure-Enhanced Close Contact Melting, *Nature Energy*, *7* (2022), 3, pp. 270-280

[11] He, Z., *et al*., Investigation of Thermal Performance of Optimized Tree-Shaped Fins in Latent Heat Storage Units, *Heat Transfer Engineering*, *46* (2025), 13-14, pp. 1136-1150
[12] Wang, Z., *et al*., Status and Challenges for Molecular Solar Thermal Energy Storage System Based Devices, *Chemical Society Reviews*, *51* (2022), 17, pp. 7313-7326

Paper submitted: March 11, 2025
Paper revised: May 22, 2025
Paper accepted: August 25, 2025

2025 Published by the Vinča Institute of Nuclear Sciences, Belgrade, Serbia.
This is an open access article distributed under the CC BY-NC-ND 4.0 terms and conditions.